Table 2. Echocardiography, Hemodynamics, and Organ Weights in Experiment 3

	MI+αGC (n=8)	MI+Anti–IL-10 Receptor Antibody (n=8)	MI+αGC+ Anti–IL-10 Receptor Antibody (n=8)
Echocardiography			
Heart rate, bpm	516±18	519±16	510±18
LVEDD, mm	4.8±0.1	5.4±0.1*	5.4±0.1*
LVESD, mm	3.9±0.1	4.6±0.1*	4.6±0.1*
FS, %	19±0.8	14.5±0.7*	15.4±0.7*
AWT, mm	0.30±0.01	0.37±0.06	0.35±0.06
PWT, mm	0.98±0.02	1.02±0.02	0.99±0.04
Hemodynamics			
Heart rate, min	518±16	487±17	515±22
Mean AoP, mm Hg	86±3	81±4	82±2
LVEDP, mm Hg	5.4±0.8	10.8±0.7*	11.4±3.3*
LV +dP/dt, mm Hg/s	10 441±661	6555±1031	7719±1284
LV –dP/dt, mm Hg/s	6847±569	4119±364	5774±1236
Organ weights			
Body wt, g	25.2±0.5	24.7±1.3	25.8±0.6
Heart wt/body wt, mg/g	6.3±0.3	8.8±0.9	6.9±0.5
Lung wt/body wt, mg/g	5.5±0.1	10.9±2.1*	7.9±1.0*
Infarct size, %	56±2	54±2	56±4

LVEDD indicates left ventricular end-diastolic diameter; LVESD, left ventricular end-systolic diameter; FS, fractional shortening; AWT, anterior wall thickness; PWT, posterior wall thickness; AoP, aortic pressure; LVEDP, left ventricular end-diastolic pressure; wt, weight. Data are mean±SEM.

*$P<0.05$ versus MI+ αGC.

LV remodeling and failure after MI. However, the precise role of various inflammatory cells and chemokines in this disease process has not been fully elucidated. iNKT cells are specialized lineage of T cells that recognize glycolipid antigens presented by the MHC class I–like molecule CD1d. The iNKT cells mediate various functions rapidly by producing a mixture of T_H1 and T_H2 cytokines and vast array of chemokines.[6] Thus, iNKT cells can function as a bridge between the innate and adaptive immune systems and orchestrate tissue inflammation. However, to our knowledge, there has been only one paper, by Olson et al, that reported the presence of iNKT cells in cardiac tissue obtained from acute Lyme carditis model.[20] Therefore, the present study was the first that demonstrated the increased infiltration of iNKT cells in post-MI hearts (Figure 1).

Effects of the Activation of iNKT Cells by αGC in Post-MI Heart

The most important finding of this study was that the activation of iNKT cells by αGC improved survival and attenuated LV remodeling and failure after MI (Figures 2 and 3 and Table 1). The beneficial effects of αGC were not attributable to its MI size-sparing effect, because the infarct size calculated as %LV circumference was comparable between MI+PBS and MI+αGC mice. Furthermore, its effects might not be attributable to those on hemodynamics, because blood pressure and heart rate were not altered (Table 1). αGC, a glycosphingolipid, is a well-known iNKT cell receptor ligand that can specifically activate iNKT cells.[13] It has been demonstrated that iNKT cells expand dramatically 2 to 3 days after in vivo treatment with αGC and return to the baseline level by approximately 9 days after treatment.[21,22] Moreover, the effects of iNKT cell stimulation may differ according to the timing of αGC administration. In the model of experimental autoimmune encephalomyelitis, early immunization with αGC protected against this disease, whereas later immunization potentiated it.[23] In the present study, αGC injection significantly enhanced iNKT cell infiltration (Figure 1) and could effectively ameliorate post-MI LV remodeling and failure (Figures 2 and 3).

Role of IL-10 in the Inhibitory Effects of iNKT Cell Activation by αGC

Another important finding of the present study was that the enhanced expression of IL-10 was involved in the inhibitory effects of iNKT cell activation against LV remodeling and failure (Table 2). These results are consistent with the previous findings that the therapeutic effects of αGC against T_H1-like autoimmune diseases include 2 mechanisms such as a shift from T_H1 toward a T_H2 pattern[9–11,23] and the induction of immunosuppressive cytokine IL-10.[9,11,12] The present study demonstrated that IL-10 was increased in noninfarcted LV from sham and MI animals in association with an increase in iNKT cells after the treatment with αGC at 7 days (Figure 6C and 6D). Interestingly, the enhanced expression of IL-10 gene by αGC persisted only in MI mice. These changes of IL-10 gene expression (Figure 6D) completely corresponded to those of iNKT cells (Figure 1B). Moreover, the inhibitory effects of αGC on LV remodeling and HF were reversed by anti–IL-10 receptor antibody and the treatment with only anti–IL-10 antibody of MI mice did not affect LV remodeling and HF (Table 2). Therefore, these data suggest that IL-10 is not associated with the development of LV remodeling and HF after MI without αGC, and IL-10 is involved in the beneficial effects of iNKT cell activation against post-MI remodeling and failure. These findings were consistent with a recent study by Krishnamurthy et al, in which LV dimension and function by echocardiography after MI did not differ between wild-type and IL-10–null mice.[24]

Possible Mechanisms of IL-10 for the Attenuation of LV Remodeling

IL-10 can inhibit the production of proinflammatory cytokines by macrophages and T_H1 cells[25,26] and directly promote the death of inflammatory cells.[27] Furthermore, beyond its suppressive effects on inflammatory gene synthesis, IL-10 also regulates extracellular matrix[28] and angiogenesis.[29] In the present study, the activation of iNKT cells by αGC decreased cardiac myocyte hypertrophy and apoptosis and inhibited interstitial fibrosis possibly through inhibiting the zymographic MMP-2 level in noninfarcted LV (Figure 4). MMP-2 is ubiquitously distributed in cardiac myocytes and fibroblasts and has been shown to play a crucial role in the

development of cardiac remodeling after MI.[30] Theoretically, an increase in MMP activity would result in a decrease in the MMP substrate, collagens, whereas an inhibition of MMP would result in an increase in collagens. However, our previous study showed that the selective disruption of the MMP-2 gene attenuated interstitial fibrosis after MI.[30] Therefore, the decrease in zymographic MMP-2 level by αGC might be involved in the attenuation of interstitial fibrosis in our model. On the other hand, MMP-9 is mainly expressed in infiltrating inflammatory cells such as neutrophils and T lymphocytes. A previous report showed that subcutaneous injection of recombinant IL-10 suppressed inflammation and attenuated LV remodeling after MI in mice by inhibiting fibrosis via suppression of HuR/MMP-9 and by enhancing capillary density through the activation of STAT3.[31] Moreover, the previous study by Burchfield et al showed that IL-10 from transplanted bone marrow mononuclear cells contributed to cardiac protection after MI in association with a decrease in T lymphocyte accumulation, reactive hypertrophy, and myocardial collagen deposition.[32] However, in the present study, zymographic MMP-9 level was not affected by αGC, which was consistent with the infiltration of lymphocyte observed by immunohistochemical staining for CD3 (Figure 5). We also measured the protein levels of HuR/MMP-9 or STAT3 in the noninfarcted LV. However, these protein levels were not affected by αGC (data not shown).

Role of Other Inflammatory Cells and Cytokines

In agreement with the increase in macrophage infiltration by αGC, MCP-1 gene expression was increased. αGC increased not only M1 macrophages but also M2 macrophages, which tune inflammatory responses and promote tissue repair.[33] Therefore, the increase in M2 macrophage might neutralize the effect of the increased M1 macrophage and MCP-1. The present study also showed that TNF-α was increased in noninfarcted LV from MI+αGC (Figure 6). TNF-α is a proinflammatory cytokine considered to be cardiotoxic and induce LV dysfunction.[34] However, in contrast, TNF-α has also protective effects during the maladaptive transition to HF.[35] Indeed, the treatment of patients with HF with either soluble TNF receptor (RENEWAL) or an anti-TNF antibody (ATTACH) could not show clinical benefits.[36,37] Therefore, the increase in TNF-α by αGC would not necessarily lead to the aggravation of LV remodeling.

Limitations

There are several limitations to be acknowledged in the present study. First, we could not directly demonstrate the location of iNKT cells by the immunohistochemical analysis using biotinylated CD1d dimer (BD Bioscience) with loading of αGC according to the previous report by Kamijyuku et al.[38] We tried the double immunohistochemical staining, using antibodies for anti–Armenian hamster TCR-β-PE (BD Bioscience) and anti-mouse NK 1.1-APC (BD Bioscience) according to the newly published paper.[39] Furthermore, we also performed in situ hybridization using digoxigenin-labeled DNA probes for mouse Vα14Jα18. Unfortunately, however, we could not detect iNKT cells in situ in the heart. Even though we defined iNKT cells within the heart by using the gene expression as well as the flow cytometric analysis, further studies are needed to overcome some technical difficulties of in situ detection and clarify this important issue. Second, the underlying mechanisms responsible for the activation of iNKT cells after MI remain to be established. To date, the endogenous ligand for iNKT cells has not been known. Based on our results using αGC, a glycosphingolipid, sphingolipid ceramide may be a crucial intermediate, since ceramide has been shown to be synthesized by long-chain fatty acids and actually increased in the heart after coronary microembolization.[40] Third, the source of IL-10 production after the stimulation of αGC remains to be determined. IL-10 has been shown to be produced by iNKT cells themselves on exogenous stimulation.[41] In addition, IL-10 can be expressed and secreted from macrophages activated by iNKT cells.[42,43] In the present study, the activation of iNKT cells by αGC injection increased the infiltration of macrophage in sham and MI mice at 7 days; however, there was no difference in it between MI+PBS and MI+αGC at 28 days (Figure 6). Therefore, the main source of IL-10 production at later phase of αGC injection would be the cells other than macrophages.

In conclusion, iNKT cells have a protective effect on LV remodeling and failure after MI via enhanced IL-10 expression. Therefore, therapies designed to activate iNKT cells may be beneficial against the development of post-MI heart failure.

Acknowledgments

We thank Kaoruko Kawai, Akiko Aita, and Miwako Fujii for excellent technical assistance.

Sources of Funding

This study was supported by grants from the Ministry of Education, Science, and Culture (17390223, 20590854, 20117004, 21390236) and Hokkaido Heart Association Grant for Research.

Disclosures

None.

References

1. Pfeffer MA, Braunwald E. Ventricular remodeling after myocardial infarction: experimental observations and clinical implications. *Circulation*. 1990;81:1161–1172.
2. Hayashidani S, Tsutsui H, Shiomi T, Ikeuchi M, Matsusaka H, Suematsu N, Wen J, Egashira K, Takeshita A. Anti-monocyte chemoattractant protein-1 gene therapy attenuates left ventricular remodeling and failure after experimental myocardial infarction. *Circulation*. 2003;108:2134–2140.
3. Varda-Bloom N, Leor J, Ohad DG, Hasin Y, Amar M, Fixler R, Battler A, Eldar M, Hasin D. Cytotoxic T lymphocytes are activated following myocardial infarction and can recognize and kill healthy myocytes in vitro. *J Mol Cell Cardiol*. 2000;32:2141–2149.
4. Shiomi T, Tsutsui H, Hayashidani S, Suematsu N, Ikeuchi M, Wen J, Ishibashi M, Kubota T, Egashira K, Takeshita A. Pioglitazone, a peroxisome proliferator-activated receptor-gamma agonist, attenuates left ventricular remodeling and failure after experimental myocardial infarction. *Circulation*. 2002;106:3126–3132.
5. Kaikita K, Hayasaki T, Okuma T, Kuziel WA, Ogawa H, Takeya M. Targeted deletion of CC chemokine receptor 2 attenuates left ventricular remodeling after experimental myocardial infarction. *Am J Pathol*. 2004;165:439–447.

6. Matsuda JL, Mallevaey T, Scott-Browne J, Gapin L. CD1d-restricted iNKT cells, the 'Swiss-Army knife' of the immune system. *Curr Opin Immunol*. 2008;20:358–368.
7. Nakai Y, Iwabuchi K, Fujii S, et al. Natural killer T cells accelerate atherogenesis in mice. *Blood*. 2004;104:2051–2059.
8. Ohmura K, Ishimori N, Ohmura Y, Tokuhara S, Nozawa A, Horii S, Andoh Y, Fujii S, Iwabuchi K, Onoe K, Tsutsui H. Natural killer T cells are involved in adipose tissues inflammation and glucose intolerance in diet-induced obese mice. *Arterioscler Thromb Vasc Biol*. 2010;30:193–199.
9. Hong S, Wilson MT, Serizawa I, Wu L, Singh N, Naidenko OV, Miura T, Haba T, Scherer DC, Wei J, Kronenberg M, Koezuka Y, Van Kaer L. The natural killer T-cell ligand alpha-galactosylceramide prevents autoimmune diabetes in non-obese diabetic mice. *Nat Med*. 2001;7:1052–1056.
10. Sharif S, Arreaza GA, Zucker P, et al. Activation of natural killer T cells by alpha-galactosylceramide treatment prevents the onset and recurrence of autoimmune Type 1 diabetes. *Nat Med*. 2001;7:1057–1062.
11. Furlan R, Bergami A, Cantarella D, Brambilla E, Taniguchi M, Dellabona P, Casorati G, Martino G. Activation of invariant NKT cells by alphaGalCer administration protects mice from MOG35–55-induced EAE: critical roles for administration route and IFN-gamma. *Eur J Immunol*. 2003;33:1830–1838.
12. Miellot A, Zhu R, Diem S, Boissier MC, Herbelin A, Bessis N. Activation of invariant NK T cells protects against experimental rheumatoid arthritis by an IL-10-dependent pathway. *Eur J Immunol*. 2005;35:3704–3713.
13. Van Kaer L. Alpha-galactosylceramide therapy for autoimmune diseases: prospects and obstacles. *Nat Rev Immunol*. 2005;5:31–42.
14. Kinugawa S, Tsutsui H, Hayashidani S, Ide T, Suematsu N, Satoh S, Utsumi H, Takeshita A. Treatment with dimethylthiourea prevents left ventricular remodeling and failure after experimental myocardial infarction in mice: role of oxidative stress. *Circ Res*. 2000;87:392–398.
15. Namba T, Tsutsui H, Tagawa H, Takahashi M, Saito K, Kozai T, Usui M, Imanaka-Yoshida K, Imaizumi T, Takeshita A. Regulation of fibrillar collagen gene expression and protein accumulation in volume-overloaded cardiac hypertrophy. *Circulation*. 1997;95:2448–2454.
16. Leuschner F, Panizzi P, Chico-Calero I, Lee WW, Ueno T, Cortez-Retamozo V, Waterman P, Gorbatov R, Marinelli B, Iwamoto Y, Chudnovskiy A, Figueiredo JL, Sosnovik DE, Pittet MJ, Swirski FK, Weissleder R, Nahrendorf M. Angiotensin-converting enzyme inhibition prevents the release of monocytes from their splenic reservoir in mice with myocardial infarction. *Circ Res*. 2010;107:1364–1373.
17. Kawano T, Cui J, Koezuka Y, Toura I, Kaneko Y, Motoki K, Ueno H, Nakagawa R, Sato H, Kondo E, Koseki H, Taniguchi M. CD1d-restricted and TCR-mediated activation of valpha14 NKT cells by glycosylceramides. *Science*. 1997;278:1626–1629.
18. Blankesteijn WM, Creemers E, Lutgens E, Cleutjens JP, Daemen MJ, Smits JF. Dynamics of cardiac wound healing following myocardial infarction: observations in genetically altered mice. *Acta Physiol Scand*. 2001;173:75–82.
19. Frangogiannis NG, Smith CW, Entman ML. The inflammatory response in myocardial infarction. *Cardiovasc Res*. 2002;53:31–47.
20. Olson CM Jr, Bates TC, Izadi H, Radolf JD, Huber SA, Boyson JE, Anguita J. Local production of IFN-gamma by invariant NKT cells modulates acute Lyme carditis. *J Immunol*. 2009;182:3728–3734.
21. Crowe NY, Uldrich AP, Kyparissoudis K, Hammond KJ, Hayakawa Y, Sidobre S, Keating R, Kronenberg M, Smyth MJ, Godfrey DI. Glycolipid antigen drives rapid expansion and sustained cytokine production by NK T cells. *J Immunol*. 2003;171:4020–4027.
22. Wilson MT, Johansson C, Olivares-Villagomez D, Singh AK, Stanic AK, Wang CR, Joyce S, Wick MJ, Van Kaer L. The response of natural killer T cells to glycolipid antigens is characterized by surface receptor down-modulation and expansion. *Proc Natl Acad Sci U S A*. 2003;100:10913–10918.
23. Jahng AW, Maricic I, Pedersen B, Burdin N, Naidenko O, Kronenberg M, Koezuka Y, Kumar V. Activation of natural killer T cells potentiates or prevents experimental autoimmune encephalomyelitis. *J Exp Med*. 2001;194:1789–1799.
24. Krishnamurthy P, Lambers E, Verma S, Thorne T, Qin G, Losordo DW, Kishore R. Myocardial knockdown of mRNA-stabilizing protein HuR attenuates post-MI inflammatory response and left ventricular dysfunction in IL-10-null mice. *FASEB J*.24:2484–2494.
25. Fiorentino DF, Zlotnik A, Vieira P, Mosmann TR, Howard M, Moore KW, O'Garra A. IL-10 acts on the antigen-presenting cell to inhibit cytokine production by Th1 cells. *J Immunol*. 1991;146:3444–3451.
26. Frangogiannis NG, Mendoza LH, Lindsey ML, Ballantyne CM, Michael LH, Smith CW, Entman ML. IL-10 is induced in the reperfused myocardium and may modulate the reaction to injury. *J Immunol*. 2000;165:2798–2808.
27. Wang P, Wu P, Siegel MI, Egan RW, Billah MM. Interleukin (IL)-10 inhibits nuclear factor kappa B (NF kappa B) activation in human monocytes. IL-10 and IL-4 suppress cytokine synthesis by different mechanisms. *J Biol Chem*. 1995;270:9558–9563.
28. Lacraz S, Nicod LP, Chicheportiche R, Welgus HG, Dayer JM. IL-10 inhibits metalloproteinase and stimulates TIMP-1 production in human mononuclear phagocytes. *J Clin Invest*. 1995;96:2304–2310.
29. Silvestre JS, Mallat Z, Duriez M, Tamarat R, Bureau MF, Scherman D, Duverger N, Branellec D, Tedgui A, Levy BI. Antiangiogenic effect of interleukin-10 in ischemia-induced angiogenesis in mice hindlimb. *Circ Res*. 2000;87:448–452.
30. Hayashidani S, Tsutsui H, Ikeuchi M, Shiomi T, Matsusaka H, Kubota T, Imanaka-Yoshida K, Itoh T, Takeshita A. Targeted deletion of MMP-2 attenuates early LV rupture and late remodeling after experimental myocardial infarction. *Am J Physiol Heart Circ Physiol*. 2003;285: H1229–H1235.
31. Krishnamurthy P, Rajasingh J, Lambers E, Qin G, Losordo DW, Kishore R. IL-10 inhibits inflammation and attenuates left ventricular remodeling after myocardial infarction via activation of STAT3 and suppression of HuR. *Circ Res*. 2009;104:e9–e18.
32. Burchfield JS, Iwasaki M, Koyanagi M, Urbich C, Rosenthal N, Zeiher AM, Dimmeler S. Interleukin-10 from transplanted bone marrow mononuclear cells contributes to cardiac protection after myocardial infarction. *Circ Res*. 2008;103:203–211.
33. Mantovani A, Sica A, Locati M. Macrophage polarization comes of age. *Immunity*. 2005;23:344–346.
34. Kubota T, McTiernan CF, Frye CS, Slawson SE, Lemster BH, Koretsky AP, Demetris AJ, Feldman AM. Dilated cardiomyopathy in transgenic mice with cardiac-specific overexpression of tumor necrosis factor-alpha. *Circ Res*. 1997;81:627–635.
35. Wang X, Oka T, Chow FL, Cooper SB, Odenbach J, Lopaschuk GD, Kassiri Z, Fernandez-Patron C. Tumor necrosis factor-alpha-converting enzyme is a key regulator of agonist-induced cardiac hypertrophy and fibrosis. *Hypertension*. 2009;54:575–582.
36. Mann DL, McMurray JJ, Packer M, et al. Targeted anticytokine therapy in patients with chronic heart failure: results of the Randomized Etanercept Worldwide Evaluation (RENEWAL). *Circulation*. 2004;109: 1594–1602.
37. Chung ES, Packer M, Lo KH, Fasanmade AA, Willerson JT. Randomized, double-blind, placebo-controlled, pilot trial of infliximab, a chimeric monoclonal antibody to tumor necrosis factor-alpha, in patients with moderate-to-severe heart failure: results of the anti-TNF Therapy Against Congestive Heart Failure (ATTACH) trial. *Circulation*. 2003;107: 3133–3140.
38. Kamijuku H, Nagata Y, Jiang X, et al. Mechanism of NKT cell activation by intranasal coadministration of alpha-galactosylceramide, which can induce cross-protection against influenza viruses. *Mucosal Immunol*. 2008;1:208–218.
39. Barral P, Sanchez-Nino MD, van Rooijen N, Cerundolo V, Batista FD. The location of splenic NKT cells favours their rapid activation by blood-borne antigen. *EMBO J*. 2012;31:2378–2390.
40. Thielmann M, Dorge H, Martin C, Belosjorow S, Schwanke U, van De Sand A, Konietzka I, Buchert A, Kruger A, Schulz R, Heusch G. Myocardial dysfunction with coronary microembolization: signal transduction through a sequence of nitric oxide, tumor necrosis factor-alpha, and sphingosine. *Circ Res*. 2002;90:807–813.
41. Sonoda KH, Faunce DE, Taniguchi M, Exley M, Balk S, Stein-Streilein J. NK T cell-derived IL-10 is essential for the differentiation of antigen-specific T regulatory cells in systemic tolerance. *J Immunol*. 2001;166:42–50.

42. Platzer C, Docke W, Volk H, Prosch S. Catecholamines trigger IL-10 release in acute systemic stress reaction by direct stimulation of its promoter/enhancer activity in monocytic cells. *J Neuroimmunol.* 2000;105:31–38.

43. Troidl C, Mollmann H, Nef H, Masseli F, Voss S, Szardien S, Willmer M, Rolf A, Rixe J, Troidl K, Kostin S, Hamm C, Elsasser A. Classically and alternatively activated macrophages contribute to tissue remodelling after myocardial infarction. *J Cell Mol Med.* 2009;13:3485–3496.

Novelty and Significance

What Is Known?

- Chronic tissue inflammation plays an important role in the development of left ventricular (LV) dysfunction and LV remodeling.
- Invariant natural killer T (iNKT) cells are a specialized lineage of T cells with NK marker. These cells produce a mixture of T_H1 and T_H2 cytokines and a vast array of chemokines to orchestrate tissue inflammation.
- iNKT cells play a protective role in experimental autoimmune and inflammatory diseases.

What New Information Does This Article Contribute?

- iNKT cells could be detected in normal heart, and their infiltration was increased in noninfarcted LV after myocardial infarction (MI).
- The activation of iNKT cells by α-galactosylceramide (αGC) improved survival and ameliorated LV remodeling and failure after MI in mice, accompanied by decreases in interstitial fibrosis, cardiomyocyte hypertrophy, and apoptosis.
- An increase in the expression of interleukin (IL)-10 by αGC was involved in the favorable effects for LV remodeling after MI.

iNKT cells regulate tissue inflammation by producing a mixture of T_H1 and T_H2 cytokines. Although chronic tissue inflammation is involved in the development of LV remodeling and failure, the pathophysiological role of iNKT cells in these processes have not been elucidated. Our study shows that infiltration of iNKT cells was increased in noninfarcted LV and their activation by αGC improved survival and ameliorated LV remodeling and failure after MI via enhanced expression of IL-10. These findings indicate a previously undescribed protective effect of iNKT cells on LV remodeling and failure after MI. Given that iNKT cells can bridge innate and adaptive immune systems, they could act as an upstream regulator of cytokine networks in the heart. Therapies designed to regulate iNKT cells and to modulate cytokine network may be beneficial in ameliorating LV remodeling and failure.

Supplemental Material

Detailed Methods

An expanded Methods section is available in the online Data Supplement at http://circres.ahajournals.org.

All procedures and animal care were approved by our institutional animal research committee and conformed to the animal care guideline for the Care and Use of Laboratory Animals in Hokkaido University Graduate School of Medicine.

Experiment 1: Time-dependent Changes of iNKT Cell Receptors in Post-MI Hearts

Animal Models

MI was created in male C57BL/6J mice, 6-8 weeks old and 20 to 25 g body weight, by ligating the left coronary artery as described previously.[1] Sham operation without ligating the coronary artery was also performed as control. MI mice were sacrificed and the hearts were excised at day 3, 7, 14 and 28 for quantitative reverse transcriptase (qRT)-PCR measurements.

Quantitative Reverse Transcriptase PCR

Total RNA was extracted from LV in sham mice and non-infarcted and infarcted LV from MI mice by using QuickGene-810 (FujiFilm, Tokyo, Japan) according to the manufacturer's instructions. cDNA was synthesized with the high capacity cDNA reverse transcription kit (Applied Biosystems, Foster City, CA). TaqMan quantitative PCR was performed with the 7300 real-time PCR system (Applied Biosystems) to amplify samples for Vα14Jα18 (a specific marker of iNKT cells).[2] This transcript was normalized to GAPDH. The primer was purchased from Applied Biosystems.

Experiment 2: Effects of iNKT Cell Activation on Post-MI Hearts

Animal Models

Sham and MI mice were created in male C57BL/6J as described in Experiment 1. Each group of mice was randomly divided into 2 groups; either α-galactosylceramide (αGC; 0.1μg/g body weight; Funakoshi Company, Ltd., Tokyo, Japan), the activator of iNKT cells, or phosphate-buffered saline (PBS) was administered via intraperitoneal injection 1 and 4 days after surgery. The concentration of αGC was chosen based on the previous study of its efficacy.[2] Thus, the experiment was performed in the following 4 groups of mice; sham+PBS (n=10), sham+αGC (n=10), MI+PBS (n=31), and MI+αGC (n=27).

Four weeks after surgery, echocardiographic studies and the hemodynamics measurement were performed. After collecting blood samples, mice were sacrificed and organ weight was measured. These measurements were performed in all survived mice (n=10 for sham+PBS, n=10 for sham+αGC, n=10 for MI+PBS, and n=16 for MI+αGC). The mice were further divided into 2 groups; for the histological analysis, including infarct size, myocyte cross-sectional area, collagen volume fraction, TUNEL staining (n=6 for each group), and for the quantitative reverse transcriptase PCR (n=4 for

each group). Additional mice were also created for MMP zymography (n=5 for each group) and for flow cytometry analysis (n=9 for each group).

A separate group of additional mice treated identically was created. One week after surgery, all mice (n=15 for each group) were sacrificed. These mice were used for immunohistochemistry (n=3 for each group), for the quantitative reverse transcriptase PCR (n=6 for each group), and for flow cytometry (n=9 for each group).

Survival

The survival analysis was performed in all 4 groups of mice. During the study period, the cages were inspected daily for deceased animals. All deceased mice were examined for the presence of MI as well as pleural effusion and cardiac rupture.

Echocardiographic and Hemodynamic Measurements

Echocardiographic and hemodynamic measurements were performed under light anesthesia with tribromoethanol/amylene hydrate (avertin; 2.5% wt/vol, 8 μL/g ip) with known short duration of action and modest cardiodepressive effects. A two-dimensional parasternal short-axis view was obtained at the levels of the papillary muscles. In general, the best views obtained with the transducer lightly applied to the mid upper left anterior chest wall. The transducer was then gently moved cephalad or caudad and angulated until desirable images were obtained. After it had been ensured that the imaging was on the axis, two-dimensional targeted M-mode tracings were recorded at a paper speed of 50mm/s. A 1.4-Fr micromanometer-tipped catheter (Millar Instruments, Houston, Texas) was inserted into the right carotid artery and then advanced into the left ventricle (LV) to measure LV pressures.

Myocardial Histopathology and Infarct Size

After mice were sacrificed, the heart was excised and dissected into right ventricle and LV including septum. LV was cut into three transverse sections; apex, middle ring, and base. From the middle ring, 5-μm sections were cut and stained with Masson's trichrome. Myocyte cross-sectional area and collagen volume fraction were determined by quantitative morphometry of tissue sections from the mid-LV as described previously.[3]

Infarct length was measured along the endocardial and epicardial surfaces in each of the cardiac sections, and the values from all specimens were summed. Infarct size (as a percentage) was calculated as total infarct circumference divided by total cardiac circumference.[1]

Myocardial Apoptosis

To detect apoptosis, tissue sections from the mid-LV were stained with the terminal deoxynucleotidyl transferase-mediated dUTP nick end-labeling (TUNEL) staining (TaKaRa Shuzo Co. Ltd., Ohtsu, Japan). The number of TUNEL positive cardiac myocyte nuclei was counted, and the data were normalized per 10^5 total nuclei identified by hematoxylin-positive staining in the same sections. The proportion of apoptotic cells was counted in the non-infarcted LV.

MMP Zymography

Zymographic MMP 2 and 9 levels in LV non-infarcted tissue was determined using gelatin zymography kit (Primary Cell Co., Ltd, Sapporo, Japan). The zymograms were digitized, and the size-fractionated bands, which indicated proteolytic levels, were measured by the integrated optical density in a rectangular region of interest.[1]

Isolation of Cardiac Mononuclear Cell and Flow Cytometry

LV tissue was harvested, minced with a fine scissors, placed in 10 ml RPMI-1640 with 5% FBS, 1 mg/ml collagenase type IV and 100 U/ml DNase I, and shaken at 37 °C for 45 min. Tissue was then triturated through nylon mesh and centrifuged (1400 rpm, 5min, 4 °C). Red blood cells were lysed with Tris-NH_4Cl solution. Cardiac mononuclear cells were isolated by density-gradient centrifugation with 33% Percoll™, as previously described.[4] Cardiac mononuclear cells from 3 mice were pooled, and subjected to flow cytometric analysis. All reagents were purchased from Sigma-Aldrich (St Louis, MO). Cardiac cell numbers were determined with Trypan blue (Wako Pure Chemical Industries, Ltd., Osaka, Japan).

The cells were incubated with 2.4G2 monoclonal antibody (mAb) to block non-specific binding of primary mAb and then reacted with Dimer X (CD1d:Ig recombinant fusion protein; BD Biosciences Pharmingen, San Diego, CA) loaded with αGC, followed by detection with phycoerythrin (PE)-conjugated anti-mouse IgG1 mAb (BD) according to the manufacturer's protocol.[5] After washing, cells were stained with a combination of fluorescein isothiocyanate (FITC)-anti-TCRβ and PE-anti-mouse IgG1 (all from BD Biosciences). Stained cells were acquired with FACS Canto II flow cytometer (BD Biosciences Immunocytometry Systems, San Jose, CA) and analyzed with FlowJo (Tommy Digital Biology, Tokyo, Japan). Propidium iodide (Sigma-Aldrich, St Louis, MO) positive cells were electronically gated as dead cells from the analysis.

RT-PCR

RNA was extracted and cDNA was synthesized were described in Experiment 1. TaqMan quantitative PCR was performed with the 7300 real-time PCR system (Applied Biosystems) to amplify samples for Vα14Jα18, CD11c (a marker of M1 macrophages), arginase-1 (a marker of M2 macrophages), MCP-1, RANTES, interferon-γ (IFN-γ), IL-4, IL-6, TNF-α, and IL-10 cDNA. These transcripts were normalized to GAPDH.

Immunohistochemistry

LV sections were immunostained with antibody against mouse MAC3 (a macrophage marker), mouse CD3 (a T cell marker), or mouse myeloperoxidase (a leucocyte marker), followed by counter-staining with hematoxylin.

Plasma Cytokines Concentration

Plasma IL-10, TNF-α, IFN-γ, IL-6, and IL-4 levels were measured by commercially

available ELISA kit (R&D systems, Inc.) in all groups.

Experiment 3: Effects of IL-10 Neutralization on αGC-Treated Post-MI Hearts

MI mice were divided into the following 3 groups of mice; MI+αGC (n=18), MI+anti-IL-10 receptor antibody (n=12), and MI+αGC+anti-IL-10 receptor antibody (n=19). αGC was administered identically as in Experiment 2. Anti-IL-10 receptor antibody (500μg/mouse, BD Pharmingen, San Diego, CA) was administered via intraperitoneal injection 1, 4, and 14 days after surgery. The concentration of anti-IL-10 receptor antibody was chosen based on the previous study of its efficacy.[6] Four weeks after surgery, echocardiographic and hemodynamics measurement were performed as described in Experiment 2. Separate set of mice from Experiment 2 was used in MI+αGC group.

Experiment 4: Specificity of αGC for NKT Cells

$V\alpha14^{+}$ NKT cell-deficient $J\alpha18^{-/-}$ (Jα18 KO) mice were provided from Dr. M. Taniguchi (RIKEN, Yokohama, Japan) and backcrossed 10 times to C57BL/6J.[7] Sham and MI mice were created in male Jα18 KO mice as described in Experiment 1. Each group of mice was treated identically to Experiment 2. Thus, the experiment was performed in the following 4 groups of mice; KO+sham+PBS, KO+sham+αGC, KO+MI+PBS, and KO+MI+αGC. One week after surgery, all mice (n=9 for each group) were sacrificed, and used for immunohistochemistry (n=3 for each group), and for the quantitative reverse transcriptase PCR (n=6 for each group). These analyses were performed as described in Experiment 2.

Statistical Analysis

Data were expressed as means ± SE. Survival analysis was performed by the Kaplan-Meier method, and between-group differences in survival were tested by the log-rank test. A between-group comparison of means was performed by 1-way ANOVA, followed by t test. The Bonferroni correction was applied for multiple comparisons of means. $P<0.05$ was considered statistically significant.

The authors had full access to and take full responsibility for the integrity of the data. All authors had read and agreed to the manuscript as written.

Supplemental Figures and Figure Legends

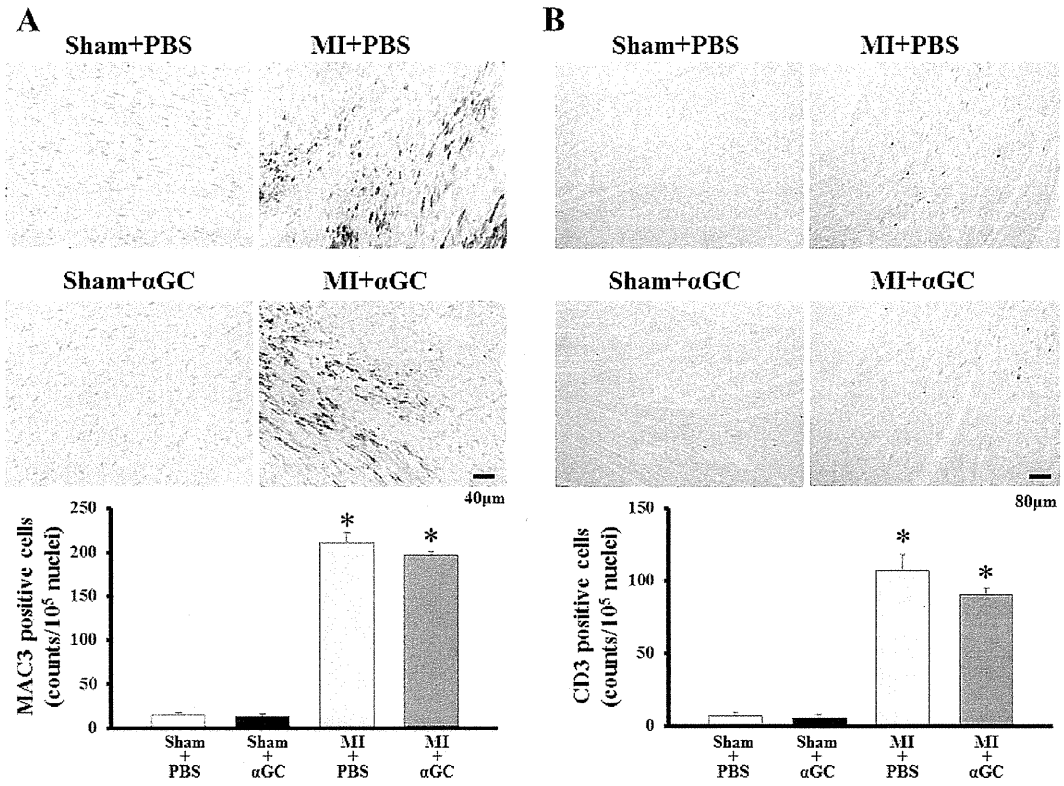

Online Figure I. Representative photomicrographs of LV cross-sections stained with (**A, upper panel**) anti MAC-3 and (**B, upper panel**) anti CD3 in KO+Sham+PBS, KO+Sham+αGC, KO+MI+PBS and KO+MI+αGC. Summary data of the numbers of (**A, lower panel**) MAC-3 and (**B, lower panel**) CD3 positive cells in the LV (n=4-8 for each). Data are means±SE. **P*<0.05 vs. Sham+PBS.

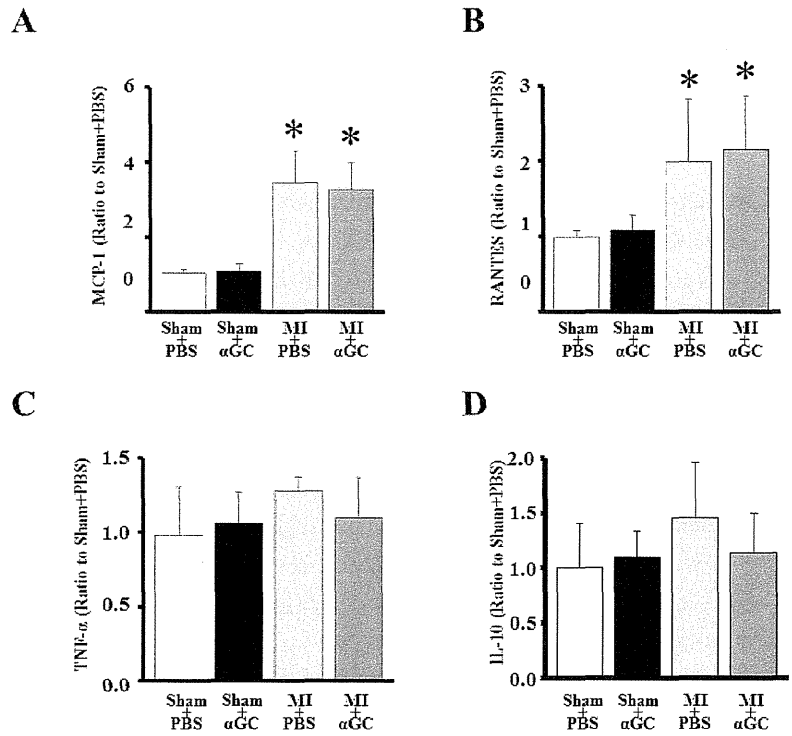

Online Figure II. Quantitative analysis of gene expression of MCP-1 (**A**), RANTES (**B**), TNF-α (**C**), and IL-10 (**D**) in the non-infarcted LV from KO mice at day 7 after surgery. Gene expression was normalized to GAPDH and depicted as the ratio to Sham+PBS. Data are expressed as means ± SE. **P*<0.05 vs. Sham+PBS.

Supplemental References

1. Kinugawa S, Tsutsui H, Hayashidani S, Ide T, Suematsu N, Satoh S, Utsumi H, Takeshita A. Treatment with dimethylthiourea prevents left ventricular remodeling and failure after experimental myocardial infarction in mice: role of oxidative stress. *Circ Res.* 2000;87:392-398.
2. Ohmura K, Ishimori N, Ohmura Y, Tokuhara S, Nozawa A, Horii S, Andoh Y, Fujii S, Iwabuchi K, Onoe K, Tsutsui H. Natural killer T cells are involved in adipose tissues inflammation and glucose intolerance in diet-induced obese mice. *Arterioscler Thromb Vasc Biol.* 2010;30:193-199.
3. Namba T, Tsutsui H, Tagawa H, Takahashi M, Saito K, Kozai T, Usui M, Imanaka-Yoshida K, Imaizumi T, Takeshita A. Regulation of fibrillar collagen gene expression and protein accumulation in volume-overloaded cardiac hypertrophy. *Circulation.* 1997;95:2448-2454.
4. Leuschner F, Panizzi P, Chico-Calero I, Lee WW, Ueno T, Cortez-Retamozo V, Waterman P, Gorbatov R, Marinelli B, Iwamoto Y, Chudnovskiy A, Figueiredo JL, Sosnovik DE, Pittet MJ, Swirski FK, Weissleder R, Nahrendorf M. Angiotensin-converting enzyme inhibition prevents the release of monocytes from their splenic reservoir in mice with myocardial infarction. *Circ Res.* 2010;107:1364-1373.
5. Nakai Y, Iwabuchi K, Fujii S, Ishimori N, Dashtsoodol N, Watano K, Mishima T, Iwabuchi C, Tanaka S, Bezbradica JS, Nakayama T, Taniguchi M, Miyake S, Yamamura T, Kitabatake A, Joyce S, Van Kaer L, Onoe K. Natural killer T cells accelerate atherogenesis in mice. *Blood.* 2004;104:2051-2059.
6. Miellot A, Zhu R, Diem S, Boissier MC, Herbelin A, Bessis N. Activation of invariant NK T cells protects against experimental rheumatoid arthritis by an IL-10-dependent pathway. *Eur J Immunol.* 2005;35:3704-3713.
7. Kawano T, Cui J, Koezuka Y, Toura I, Kaneko Y, Motoki K, Ueno H, Nakagawa R, Sato H, Kondo E, Koseki H, Taniguchi M. CD1d-restricted and TCR-mediated activation of valpha14 NKT cells by glycosylceramides. *Science.* 1997;278:1626-1629.

Circulation Journal
Official Journal of the Japanese Circulation Society
http://www.j-circ.or.jp

ORIGINAL ARTICLE
Renal Disease

Renal Tubulointerstitial Damage Is Associated With Short-Term Cardiovascular Events in Patients With Myocardial Infarction

Akira Funayama, MD; Tetsuro Shishido, MD; Takehiko Miyashita, MD; Shunsuke Netsu, MD; Yoichiro Otaki, MD; Takanori Arimoto, MD; Hiroki Takahashi, MD; Takuya Miyamoto, MD; Tetsu Watanabe, MD; Tsuneo Konta, MD; Isao Kubota, MD

Background: Urinary β2 microglobulin (U-β2MG) is a more sensitive and accurate marker of tubulointerstitial damage. The etiology of glomerular damage is related to the occurrence of major adverse cardiovascular events (MACE) in patients with myocardial infarction (MI); however, the prognostic importance of tubulointerstitial damage in patients with ST-segment elevation MI (STEMI) has not been established. The aim of this study was to elucidate whether renal tubulointerstitial damage is associated with the occurrence of MACE in patients after STEMI undergoing percutaneous coronary intervention.

Methods and Results: The degree of renal tubulointerstitial damage was evaluated by measuring the U-β2MG level in 89 consecutive STEMI patients. There were 22 MACEs during the follow-up period. Patients with MACE had higher U-β2MG levels than those without MACE, and the U-β2MG level was an independent predictor for MACE. A Kaplan-Meier analysis revealed that the group with higher U-β2MG levels corrected for urinary creatinine was associated with a greater risk for MACE.

Conclusions: An elevated U-β2MG level was associated with the occurrence of MACE in STEMI patients who underwent PCI. Renal tubulointerstitial damage is therefore considered to be associated with the occurrence of MACE. (*Circ J* 2013; **77:** 484–489)

Key Words: Percutaneous coronary intervention; Secondary prevention; Tubulointerstitial damage

The prevalence of chronic kidney disease (CKD) is an independent risk factor for cardiovascular disease.[1,2] The most predictive factors for progression to renal dysfunction are glomerular injury and tubulointerstitial damage.[3] Urinary β2 microglobulin (U-β2MG) is a more sensitive and accurate marker of tubulointerstitial damage,[4] and its excretion predicts a rapid 1-year decline in renal function. Thus, an increased U-β2MG level is an independent risk factor for rapid renal deterioration.[5,6]

The etiology of glomerular damage is related to the occurrence of major adverse cardiovascular events (MACE) in patients with myocardial infarction (MI).[7] Renal tubular damage is associated with impaired outcomes in chronic heart failure patients,[8,9] even when the estimated glomerular filtration rate (eGFR) is normal,[10] implying that tubulointerstitial damage might be a risk factor for mortality after MI. However, the prognostic importance of tubulointerstitial damage in patients with ST-segment elevation MI (STEMI) has not been established. The aim of this study was to examine whether the level of U-β2MG, a marker for tubulointerstitial damage, is associated with the onset of MACE in patients with STEMI after successful percutaneous coronary intervention (PCI).

Methods

Study Population

This study evaluated 95 consecutive patients who underwent PCI between May 2008 and April 2011 for STEMI within 24 h of the onset of symptoms at the Yamagata University Hospital. PCI was successfully carried out in all patients with the use of bare metal stents. STEMI was diagnosed by (1) typical chest pain lasting >30 min, (2) ST-segment elevation in at least 2 contiguous leads or left bundle-branch block on ECG, and (3) typical increase and decrease in the serum creatine kinase concentration above twice the upper limit of normal. The exclusion criteria were eGFR <30 ($ml \cdot min^{-1} \cdot 1.73 m^{-2}$), acute kidney injury[11] (within 48 h, increase in serum creatinine concentration of ≥0.5 mg/dl from baseline), and data unavailability

Received May 15, 2012; revised manuscript received August 24, 2012; accepted September 18, 2012; released online October 31, 2012 Time for primary review: 13 days
Department of Cardiology, Pulmonology, and Nephrology, Yamagata University School of Medicine, Yamagata, Japan
Mailing address: Tetsuro Shishido, MD, Department of Cardiology, Pulmonology, and Nephrology, Yamagata University School of Medicine, 2-2-2 Iida-Nishi, Yamagata 990-9585, Japan. E-mail: tshishid@med.id.yamagata-u.ac.jp
ISSN-1346-9843 doi:10.1253/circj.CJ-12-0640

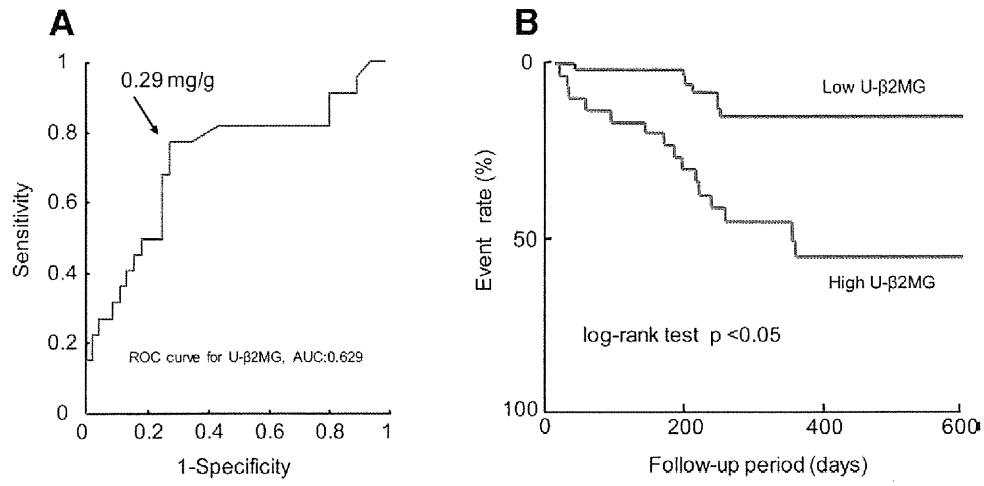

Figure 1. (A) Receiver-operating characteristic (ROC) curve analysis of UBCR. (B) Patients were divided into 2 groups based on the UBCR cut-off value as determined by the ROC curves: low UBCR group (n=59), high UBCR group (n=30). Kaplan-Meier analysis of the event rate among the 2 groups. AUC, area under the ROC curve; UBCR, urine β2 microglobulin-creatinine ratio.

(n=6). Therefore 89 patients were included in the present study. Written informed consent was given by all the patients before the study. The protocol was approved by the institutional human investigations committee.

U-β2MG and Other Biochemical Analyses

U-β2MG was measured in a single spot urine specimen collected at admission after PCI. U-β2MG levels corrected for urinary creatinine (UBCR) were used for all analyses.[5] The general biochemical parameters were measured using routine laboratory methods. The eGFR was calculated using the abbreviated Modification of Diet in Renal Disease equation with the Japanese coefficient as described previously.[12,13]

Gensini Score

To assess the severity of coronary artery disease (CAD), we used the Gensini scoring system:[14] coronary artery score=sum of all segment scores (where each segment score equals segment weighting factor multiplied by severity score). Severity scores assigned to the specific percentage luminal diameter reduction of the coronary artery segment are 32 for 100%, 16 for 99%, 8 for 90%, 4 for 75%, 2 for 50%, and 1 for 25%.

Endpoints and Follow-up

No patients were lost to follow-up (mean follow-up period, 342±220 days) after admission. Clinical follow-up data were obtained from either outpatient record reviews or telephone interviews. The occurrence of MACE included cardiac death, rehospitalization for congestive heart failure, target lesion revascularization (TLR), target vessels revascularization or disabling stroke.

Statistical Analysis

The results are presented as the mean±SD for continuous variables and as percentages of the total number of patients for categorical variables. Skewed values are expressed as medians and the interquartile range. Student's unpaired t-test and the chi-square test were used for comparisons of continuous and categorical variables, respectively. If the data were not normally distributed, then the Mann-Whitney U test was used. A Cox proportional-hazards regression analysis was performed to evaluate the associations between MACE and measurements. The cardiac-event-free curve was computed according to the Kaplan-Meier method and compared using the log-rank test. The optimal cut-off value for UBCR was determined as that with the largest sum of sensitivity plus specificity on each of the receiver-operating characteristic (ROC) curves. The cut-off value of UBCR (0.29 mg/g) was determined by ROC curves as shown in Figure 1A. Only variables with P<0.05 according to univariate Cox regression analysis were entered into the multivariate Cox regression analysis. All P values were 2-sided, and P<0.05 was considered to be significant.

Results

The clinical characteristics of the patients with and without MACE are shown in Table 1. Patients with MACE had lower left ventricular ejection fraction (LVEF) (47.8±14.4 vs. 57.4±9.8, P<0.05), Thrombolysis In Myocardial Infarction (TIMI) flow after the procedure (0/0/6/16 vs. 0/0/5/62 in TIMI flow 0, 1, 2, and 3, respectively, P<0.05), higher Gensini score (70.5±37.4 vs. 53.7±24.9, P<0.05), higher urinary N-acetyl-β-D-glucosaminidase (NAG; 16.5±12.0 vs. 11.9±6.8, P<0.05) and UBCR levels [0.427 (0.278–2.037) vs. 0.149 (0.052–0.264), P<0.05] in comparison with those without MACE. Patients with MACE were less frequently administered angiotensin-converting enzyme inhibitors (ACEIs) or angiotensin II receptor blockers (ARBs) [17 (77%) vs. 65 (97%) P<0.05] and statins [15 (68%) and 60 (90%), P<0.05] than those without MACE. Other variables, including age, sex, numbers of patients (those with hypertension, hyperlipidemia, and diabetes mellitus), eGFR (71.5±19.3 vs. 76.7±22.9), prevalence of proteinuria [5 (23%) vs. 13 (19%)], urinary pH, and contrast media volume on PCI [133 (110–210) vs. 150 (100–170)] were not different between patients with and without MACE. There were no significant differences in the use of diuretics and/or nonsteroidal antiinflammatory drugs between the 2 groups in the present study.

Univariate and multivariate Cox proportional-hazards re-

Table 1. Clinical Characteristics of the Study Patients

	MACE (–) (n=67)	MACE (+) (n=22)	P value
Age, years	65.9±11.8	66.2±10.3	0.91
Men, n (%)	55 (82)	18 (82)	0.98
Hypertension, n (%)	49 (73)	17 (77)	0.70
Dyslipidemia, n (%)	35 (52)	14 (64)	0.35
Diabetes mellitus, n (%)	19 (28)	6 (27)	0.92
LVEF, %	57.4±9.8	47.8±14.4	<0.05
Medications			
Aspirin, n (%)	67 (100)	22 (100)	–
Clopidogrel, n (%)	66 (99)	21 (95)	0.44
ACEIs or ARBs, n (%)	65 (9)	17 (77)	<0.05
β-blockers, n (%)	39 (58)	9 (41)	0.16
Statins, n (%)	60 (90)	15 (68)	<0.05
Laboratory data			
Peak creatine kinase, IU	2,379 (1,208–4,006)	2,533 (1,322–5,258)	0.38
Serum creatinine, mg/dl	0.80±0.27	0.86±0.24	0.38
eGFR, ml·min^{-1}·1.73 m^{-2}	76.7±22.9	71.5±19.3	0.35
Proteinuria, n (%)	13 (19)	5 (23)	0.06
UBCR, mg/g	0.149 (0.052–0.264)	0.427 (0.278–2.037)	<0.05
Urinary NAG, U/L	11.9±6.8	16.5±12.0	<0.05
Urinary pH	6.51±0.88	6.21±0.75	0.15
Infarct-related vessel, n (%)			0.86
LAD	38 (57)	11 (50)	
LCX	5 (7)	2 (9)	
RCA	24 (36)	9 (41)	
No. of diseased vessels (1/2/3)	57/7/3	17/4/1	0.79
Thrombectomy, n (%)	60 (89)	19 (86)	0.69
No. of stents	1.13±0.43	1.18±0.16	0.66
Stent diameter, mm	3.52±0.43	3.37±0.35	0.14
Stent length, mm	20.3±4.71	21.0±3.6	0.52
TIMI flow before procedure (0/1/2/3)	54/8/2/3	21/0/1/0	0.24
TIMI flow after procedure (0/1/2/3)	0/0/5/62	0/0/6/16	<0.05
Contrast media volume on PCI (ml)	150 (100–170)	133 (110–210)	0.92
Gensini score	53.7±24.9	70.5±37.4	<0.05

ACEIs, angiotensin-converting enzyme inhibitors; ARBs, angiotensin II receptor blockers; eGFR, estimated glomerular filtration rate; LAD, left descending artery; LCX, left circumflex artery; LVEF, left ventricular ejection fraction; MACE, major adverse cardiovascular events; NAG, N-acetyl-β-D-glucosaminidase; PCI, percutaneous coronary intervention; RCA, right coronary artery; TIMI, Thrombolysis In Myocardial Infarction; UBCR, urine β2 microglobulin-creatinine ratio.

Table 2. Factors Associated With MACE (Multivariate Cox Proportional-Hazards Analysis)

Factors	Multivariate		
	HR	95% CI	P value
LVEF*	0.602	0.249–1.442	0.26
ACEIs or ARBs	0.116	0.016–0.859	<0.05
Statins	0.492	0.056–4.343	0.52
UBCR*	7.714	1.405–42.39	<0.05
Urinary NAG*	1.571	0.771–3.216	0.21
TIMI flow after procedure	5.272	1.384–20.076	<0.05

*Per 1-SD increase.
CI, confidence interval; HR, hazard ratio; SD, standard deviation. Other abbreviations as in Table 1.

gression analyses were performed to determine the risk factors for predicting MACE. The univariate analysis revealed that the UBCR level was significantly associated with the occurrence of MACE. Variables with P<0.05 in the univariate analysis were entered into the multivariate Cox proportional hazards analysis (Table 2). The use of ACEIs or ARBs [hazard ratio (HR) 0.116, 95% confidence interval (CI) 0.016–0.589, P<0.05], TIMI flow after procedure (HR 5.272, 95% CI 1.384–20.076, P<0.05) and UBCR (HR 7.714, 95% CI 1.405–42.39, P<0.05) were the independent predictors of MACE.

The patients were divided into 2 groups based on the UBCR cut-off values determined by ROC curves (Figure 1A): high UBCR group (n=30) and low UBCR group (n=59). Kaplan-Meier analysis demonstrated that the high UBCR group had a significantly higher event rate than the low UBCR group (Figure 1B). The high UBCR group had significantly greater Gensini scores than the low UBCR group (67.3±33.9 vs. 53.0±25.4, P<0.05) (Figure 2A). The level of serum creatinine at 6 months after discharge was significantly higher in the high UBCR group than in the low UBCR group. The eGFR after discharge was significantly lower in the high UBCR group than in the low UBCR group. However, there were no significant differences in the level of serum creatinine or the eGFR

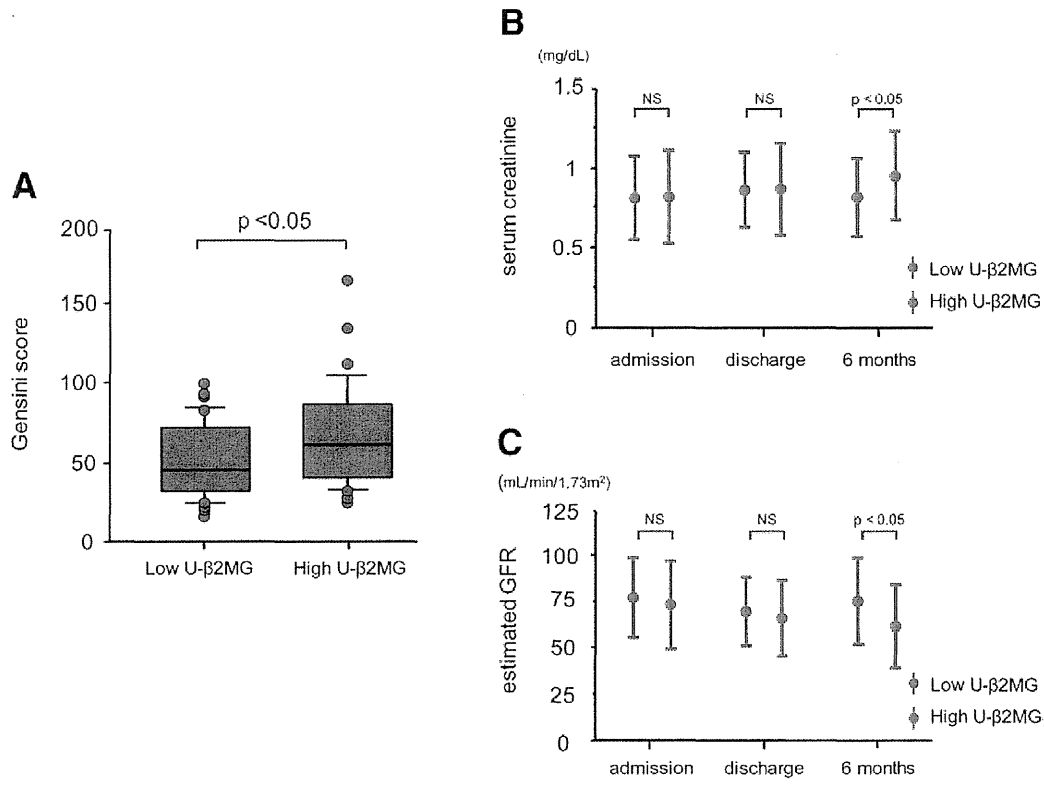

Figure 2. (A) Gensini score comparison between high and low UBCR groups at admission. (B,C) Changes in renal function: serum creatinine concentration and eGFR over time (at admission, discharge and after discharge) in the high and low UBCR groups at admission. eGFR, estimated glomerular filtration rate; UBCR, urine β2 microglobulin-creatinine ratio.

between the high and low UBCR groups at admission and discharge (Figures 2B,C).

Discussion

The present study found the UBCR level was increased in patients with MACE. Multivariate Cox proportional hazard regression analysis demonstrated the UBCR level to be an independent and strong factor that could predict the risk of MACE in patients with STEMI.

It is widely accepted that both glomerular injury and tubulointerstitial damage are involved in the progression to renal dysfunction, which is associated with progressive cardiovascular disease.[15,16] Although the UBCR level was increased in patients with MACE, there was no difference in the eGFR between patients with and without MACE. One possible reason for this result is that the causes of renal tubular damage are different from those of decreased eGFR, and those differences might be associated with the occurrence of MACE.[4] β2MG is readily filtered through the glomerulus and is completely reabsorbed by the proximal tubules. The reabsorption of β2MG is impaired when brush border cells in the proximal tubules are damaged, leading to increased U-β2MG excretion.[4,17] Another possibility is that the sensitivity to detect silent renal insufficiency might differ between eGFR and UBCR. Importantly, the prevalence of increased UBCR levels (≥300 μg/g creatinine) is higher than the prevalence of renal insufficiency diagnosed by the presence of albuminuria or decreased eGFR,[5] indicating that the UBCR level might be superior for stratifying the risk for MACE in STEMI patients after PCI.

Although several reports have demonstrated the importance of evaluating proximal tubular injury in predicting the development of renal insufficiency,[18,19] the importance of tubular damage in patients with STEMI has not been established. We found that proximal tubular damage evaluated by the level of UBCR was an independent predictor of MACE. Tubular damage is thought to be triggered by renal hypoxia induced by reduced renal perfusion, inflammation, and hypertension.[3,20,21] Fujii et al have showed the involvement of inflammation during tubulointerstitial injury.[22] Moreover, Tran et al have demonstrated the association of systemic inflammation in regulating global and tubular damage.[23] Therefore, we speculate that evaluation of tubular damage in STEMI patients contributes to the assessment of vascular inflammation, which is strongly associated with MACE.

Tubular injury is both a marker and a mediator of CKD progression,[3,24] The cardiovascular events associated with atherosclerosis are more often fatal in patients with CKD than in individuals without CKD.[25] It has been reported that the most predictive factor for progression to CKD is not only the etiology of glomerular injury, but also the degree of tubulointerstitial damage.[3] The present study showed that a high UBCR was associated with worsening renal function after discharge. In addition, the present study showed that a high UBCR at ad-

mission was associated with the severity of CAD and the occurrence of MACE. Therefore, it is important to attenuate the tubulointerstitial damage of patients after STEMI even if serum creatinine and eGFR are preserved. The key role of inflammation and oxidative stress in the pathogenesis of atherosclerosis and acute MI has become increasingly apparent in recent years, based on the results of experimental, epidemiologic and clinical studies.[26,27] Previous studies have shown that tubulointerstitial damage is associated with factors such as oxidative stress and inflammation. The renin-angiotensin system is one of the most important causes of producing oxidative stress and inflammation of the renal tubules.[3] Interestingly, recent studies have reported that ACEIs and angiotensin II type 1 (AT1) receptor blockade reduced tubular damage.[28–30] ACEIs and AT1 receptor blockers may be of potential value in patients with high UBCR among patients with STEMI, because we found that patients with MACE were less frequently administered ACEIs or ARBs compared with those without MACE; however, further research is required to demonstrate that the use of those drugs has the potential to prevent tubulointerstitial damage in patients who undergo PCI after STEMI.

The current study measured urinary NAG in addition to UBCR. The urinary NAG levels were not an independent risk factor for predicting MACE in this study, although patients with MACE demonstrated a trend toward higher levels of urinary NAG in comparison with those without MACE. Although the cause of β2MG appearance in the urine is dysfunctional absorption in the tubules, urinary NAG is released as a result of direct renal tubular injury,[4] although the detailed mechanism is still unknown, beyond these differences already discussed. Of note, UBCR has been postulated to be superior to urinary NAG for predicting the prognosis in idiopathic membranous nephropathy.[4] There is increasing evidence that urinary liver-type fatty acid binding protein (L-FABP) is a new marker for tubulointerstitial damage.[18,19] Because the current study did not evaluate the levels of L-FABP in this series, a comparison between UBCR and L-FABP is therefore still required in a future study.

The current study had a comparatively large population of MACE patients because it included TLR. The UBCR levels of patients with MACE were significantly higher than in those without MACE, even if the patients with TLR in MACE are excluded (n=12), and the UBCR levels were almost the same at the time of rehospitalization in TLR patients (data not shown). Therefore, the measurement of UBCR at admission may be a highly reliable method of risk stratifying patients with MI after PCI.

Recently, Ishibashi et al have shown that pravastatin attenuates proximal tubular cell apoptosis by inhibiting the expression of oxidative stress and advanced glycation endproducts.[31] Erythropoietin, some statins and calcium-channel blockers (CCBs) protect against tubulointerstitial injury.[31–34] However, the these drugs to reduce UBCR and which statins or CCBs have clinical benefit for tubulointerstitial damage remains unknown, and further study is required to demonstrate which drugs have the potential to preserve and improve tubular damage in STEMI patients.

In this study, coronary risk factors such as hypertension, hyperlipidemia, and diabetes mellitus were not associated with the rate of MACE after STEMI. Therefore, further studies including a large number of patients are needed to investigate the relationship between classical risk factors and tubulointerstitial damage.

Conclusions

The current data suggest that the UBCR level might be superior for stratifying the risk for MACE in STEMI patients who undergo PCI. The results of this study demonstrate that renal tubulointerstitial damage is associated with short-term cardiovascular events in patients with MI. Further studies with a larger number of patients and a longer follow-up are thus required to evaluate the usefulness of the U-β2MG level for predicting MACE.

Acknowledgments

Funding: This work was supported in part by a grants-in-aid for Scientific Research (Nos. 21590923 and 24659380 to I.K., and 23790830 to T.S.) from the Ministry of Education, Science, Sports, and Culture, Japan, and a grant-in-aid from the 21st Global Century Center of Excellence (COE) program of the Japan Society for the Promotion of Science to I.K. T.S. was supported by the Japan Heart Foundation Research Grant. The funders had no role in the study design, data collection and analysis, decision to publish, or preparation of the manuscript.

Disclosures

The authors declare no conflicts of interest with regard to this study.

References

1. Ueshima K, Oba K, Yasuno S, Fujimoto A, Tanaka S, Ogihara T, et al. Influence of coronary risk factors on coronary events in Japanese high-risk hypertensive patients: Primary and secondary prevention of ischemic heart disease in a subanalysis of the Candesartan Antihypertensive Survival Evaluation in Japan (CASE-J) trial. *Circ J* 2011; **75:** 2411–2416.
2. Kiyosue A, Hirata Y, Ando J, Fujita H, Morita T, Takahashi M, et al. Plasma cystatin C concentration reflects the severity of coronary artery disease in patients without chronic kidney disease. *Circ J* 2010; **74:** 2441–2447.
3. Nangaku M. Chronic hypoxia and tubulointerstitial injury: A final common pathway to end-stage renal failure. *J Am Soc Nephrol* 2006; **17:** 17–25.
4. Hofstra JM, Deegens JK, Willems HL, Wetzels JF. Beta-2-microglobulin is superior to N-acetyl-beta-glucosaminidase in predicting prognosis in idiopathic membranous nephropathy. *Nephrol Dial Transplant* 2008; **23:** 2546–2551.
5. Kudo K, Konta T, Mashima Y, Ichikawa K, Takasaki S, Ikeda A, et al. The association between renal tubular damage and rapid renal deterioration in the Japanese population: The Takahata study. *Clin Exp Nephrol* 2011; **15:** 235–241.
6. Ikeda A, Konta T, Takasaki S, Hao Z, Suzuki K, Sato H, et al. In a non-diabetic Japanese population, the combination of macroalbuminuria and increased urine beta 2-microglobulin predicts a decline of renal function: The Takahata study. *Nephrol Dial Transplant* 2009; **24:** 841–847.
7. Smith GL, Masoudi FA, Shlipak MG, Krumholz HM, Parikh CR. Renal impairment predicts long-term mortality risk after acute myocardial infarction. *J Am Soc Nephrol* 2008; **19:** 141–150.
8. Damman K, Masson S, Hillege HL, Maggioni AP, Voors AA, Opasich C, et al. Clinical outcome of renal tubular damage in chronic heart failure. *Eur Heart J* 2011; **32:** 2705–2712.
9. Damman K, van Veldhuisen DJ, Navis G, Voors AA, Hillege HL. Urinary neutrophil gelatinase associated lipocalin (NGAL), a marker of tubular damage, is increased in patients with chronic heart failure. *Eur J Heart Fail* 2008; **10:** 997–1000.
10. Damman K, Van Veldhuisen DJ, Navis G, Vaidya VS, Smilde TD, Westenbrink BD, et al. Tubular damage in chronic systolic heart failure is associated with reduced survival independent of glomerular filtration rate. *Heart* 2010; **96:** 1297–1302.
11. Maioli M, Toso A, Leoncini M, Micheletti C, Bellandi F. Effects of hydration in contrast-induced acute kidney injury after primary angioplasty: A randomized, controlled trial. *Circ Cardiovasc Interv* 2011; **4:** 456–462.
12. Funayama A, Shishido T, Netsu S, Ishino M, Sasaki T, Katoh S, et al. Serum pregnancy-associated plasma protein a in patients with heart failure. *J Card Fail* 2011; **17:** 819–826.
13. Suzuki S, Shishido T, Ishino M, Katoh S, Sasaki T, Nishiyama S, et al. 8-Hydroxy-2'-deoxyguanosine is a prognostic mediator for cardiac event. *Eur J Clin Invest* 2011; **41:** 759–766.

14. Gensini GG. A more meaningful scoring system for determining the severity of coronary heart disease. *Am J Cardiol* 1983; **51:** 606.
15. Arnlov J, Evans JC, Meigs JB, Wang TJ, Fox CS, Levy D, et al. Low-grade albuminuria and incidence of cardiovascular disease events in nonhypertensive and nondiabetic individuals: The Framingham Heart Study. *Circulation* 2005; **112:** 969–975.
16. Klausen KP, Scharling H, Jensen G, Jensen JS. New definition of microalbuminuria in hypertensive subjects: Association with incident coronary heart disease and death. *Hypertension* 2005; **46:** 33–37.
17. Branten AJ, du Buf-Vereijken PW, Klasen IS, Bosch FH, Feith GW, Hollander DA, et al. Urinary excretion of beta2-microglobulin and IgG predict prognosis in idiopathic membranous nephropathy: A validation study. *J Am Soc Nephrol* 2005; **16:** 169–174.
18. Kamijo-Ikemori A, Sugaya T, Yasuda T, Kawata T, Ota A, Tatsunami S, et al. Clinical significance of urinary liver-type fatty acid-binding protein in diabetic nephropathy of type 2 diabetic patients. *Diabetes Care* 2011; **34:** 691–696.
19. Matsui K, Kamijo-Ikemori A, Sugaya T, Yasuda T, Kimura K. Usefulness of urinary biomarkers in early detection of acute kidney injury after cardiac surgery in adults. *Circ J* 2012; **76:** 213–220.
20. Mazzali M, Jefferson JA, Ni Z, Vaziri ND, Johnson RJ. Microvascular and tubulointerstitial injury associated with chronic hypoxia-induced hypertension. *Kidney Int* 2003; **63:** 2088–2093.
21. Matsumoto M, Tanaka T, Yamamoto T, Noiri E, Miyata T, Inagi R, et al. Hypoperfusion of peritubular capillaries induces chronic hypoxia before progression of tubulointerstitial injury in a progressive model of rat glomerulonephritis. *J Am Soc Nephrol* 2004; **15:** 1574–1581.
22. Fujiu K, Manabe I, Nagai R. Renal collecting duct epithelial cells regulate inflammation in tubulointerstitial damage in mice. *J Clin Invest* 2011; **121:** 3425–3441.
23. Tran M, Tam D, Bardia A, Bhasin M, Rowe GC, Kher A, et al. PGC-1alpha promotes recovery after acute kidney injury during systemic inflammation in mice. *J Clin Invest* 2011; **121:** 4003–4014.
24. Risdon RA, Sloper JC, De Wardener HE. Relationship between renal function and histological changes found in renal-biopsy specimens from patients with persistent glomerular nephritis. *Lancet* 1968; **2:** 363–366.
25. Drueke TB, Massy ZA. Atherosclerosis in CKD: Differences from the general population. *Nat Rev Nephrol* 2010; **6:** 723–735.
26. Griendling KK, FitzGerald GA. Oxidative stress and cardiovascular injury. Part I: Basic mechanisms and in vivo monitoring of ROS. *Circulation* 2003; **108:** 1912–1916.
27. Levonen AL, Vahakangas E, Koponen JK, Yla-Herttuala S. Antioxidant gene therapy for cardiovascular disease: Current status and future perspectives. *Circulation* 2008; **117:** 2142–2150.
28. Norman JT, Stidwill R, Singer M, Fine LG. Angiotensin II blockade augments renal cortical microvascular pO2 indicating a novel, potentially renoprotective action. *Nephron Physiol* 2003; **94:** 39–46.
29. Manotham K, Tanaka T, Matsumoto M, Ohse T, Miyata T, Inagi R, et al. Evidence of tubular hypoxia in the early phase in the remnant kidney model. *J Am Soc Nephrol* 2004; **15:** 1277–1288.
30. Shishido T, Konta T, Nishiyama S, Miyashita T, Miyamoto T, Takasaki S, et al. Suppressive effects of valsartan on microalbuminuria and CRP in patients with metabolic syndrome (Val-Mets). *Clin Exp Hypertens* 2011; **33:** 117–123.
31. Ishibashi Y, Yamagishi SI, Matsui T, Ohta K, Tanoue R, Takeuchi M, et al. Pravastatin inhibits advanced glycation end products (AGEs)-induced proximal tubular cell apoptosis and injury by reducing receptor for AGEs (RAGE) level. *Metabolism* 2012; **61:** 1067–1072.
32. Ikee R, Kobayashi S, Saigusa T, Namikoshi T, Yamada M, Hemmi N, et al. Impact of hypertension and hypertension-related vascular lesions in IgA nephropathy. *Hypertens Res* 2006; **29:** 15–22.
33. Nakamura T, Sugaya T, Kawagoe Y, Suzuki T, Ueda Y, Koide H, et al. Azelnidipine reduces urinary protein excretion and urinary liver-type fatty acid binding protein in patients with hypertensive chronic kidney disease. *Am J Med Sci* 2007; **333:** 321–326.
34. Sharples EJ, Patel N, Brown P, Stewart K, Mota-Philipe H, Sheaff M, et al. Erythropoietin protects the kidney against the injury and dysfunction caused by ischemia-reperfusion. *J Am Soc Nephrol* 2004; **15:** 2115–2124.

Advance Publication by-J-STAGE

Circulation Journal
Official Journal of the Japanese Circulation Society
http://www.j-circ.or.jp

Gender Differences in Clinical Characteristics, Treatment and Long-Term Outcome in Patients With Stage C/D Heart Failure in Japan

– Report From The CHART-2 Study –

Yasuhiko Sakata, MD, PhD; Satoshi Miyata, PhD; Kotaro Nochioka, MD, PhD; Masanobu Miura, MD, PhD; Tsuyoshi Takada, MD; Soichiro Tadaki, MD; Jun Takahashi, MD, PhD; Hiroaki Shimokawa, MD, PhD

Background: The gender differences in patients with chronic heart failure (CHF) remain to be fully elucidated in the Japanese population.

Methods and Results: We examined gender differences in clinical characteristics, treatment and long-term outcome in 4,736 consecutive CHF patients in stage C/D (mean age, 69 years) out of 10,219 patients registered in the CHF Registry, named CHART-2 Study (NCT 00418041). Compared with male patients (68%, n=3,234), female patients (32%, n=1,502) were 3.8 years older and had lower prevalence of ischemic heart disease, diabetes, smoking, myocardial infarction and cancer. At baseline, women had higher prevalence of preserved left ventricular function but had higher NYHA functional class and increased brain natriuretic peptide level. In women, aspirin, β-blockers and statins were less frequently used and diuretics were more frequently used. Crude mortality rate was similar between the genders during the median 3.1-year follow-up (52.4/1,000 and 47.3/1,000 person-years for women and men, respectively, P=0.225). On multivariate Cox regression analysis, women had a reduced risk of mortality (adjusted HR, 0.791; 95% CI: 0.640–0.979, P=0.031).

Conclusions: Substantial gender differences exist in stage C/D CHF patients in real-world practice in Japan. Although female CHF patients had better survival than male patients after adjustment for baseline differences, crude mortality rate was similar between the genders, possibly reflecting relatively severer clinical manifestations in women.

Key Words: Gender difference; Heart failure; Observational study; Prognosis

It has been reported that women with chronic heart failure (CHF) have better survival than men in general.[1–11] The Framingham Study reported that among the 5,192 subjects without CHF aged 30–62 at the time of entry in 1949,[1] overt heart failure (HF) developed in 142 during the 16-year follow-up, that the incidence rate was greater in men than in women and that the probability of death within 5 years after onset of HF was 62% in men and 42% in women.[1] After this report, a number of studies have been conducted that also found better survival in female patients compared with male patients,[2–11] in the broad spectrum of HF, including advanced CHF[7] and HF with preserved left ventricular (LV) ejection fraction (HFpEF).[10,11]

Editorial p ????

In Japan, the number of CHF patients has been rapidly increasing along with the advancement of the aging society, particularly in women.[12,13] It remains to be fully elucidated, however, whether gender differences exist among Japanese CHF patients. Thus, in the present study, we addressed this important issue using a CHF registry database, named Chronic Heart Failure Analysis and Registry in the Tohoku District-2 (CHART-2), a prospective multicenter observational study, in

Received August 5, 2013; revised manuscript received October 24, 2013; accepted October 29, 2013; released online December 6, 2013
Time for primary review: 23 days

Departments of Cardiovascular Medicine and Evidence-based Cardiovascular Medicine, Tohoku University Graduate School of Medicine, Sendai, Japan

The Guest Editor for this article was Hiroyuki Tsutsui, MD.

Mailing address: Yasuhiko Sakata, MD, PhD, Department of Cardiovascular Medicine, Tohoku University Graduate School of Medicine, 1-1 Seiryo-machi, Aoba-ku, Sendai 980-8574, Japan. E-mail: sakatayk@cardio.med.tohoku.ac.jp

ISSN-1346-9843 doi:10.1253/circj.CJ-13-1009

Table 1. **Baseline Characteristics**

	Male (n=3,234)	Female (n=1,502)	P-value
Age (years)	67.7±12.1	71.5±12.3	<0.001
Body weight (kg)	64.5±11.3	52.1±11.2	<0.001
Height (cm)	163.7±7.1	149.4±6.8	<0.001
Body mass index (kg/m²)	24±3.5	23.3±4.5	<0.001
NYHA functional class			<0.001
I	841 (26.1)	251 (16.8)	
II	2,080 (64.6)	1,011 (67.6)	
III	277 (8.6)	217 (14.5)	
IV	23 (0.7)	16 (1.1)	
Baseline cardiovascular disease			
Ischemic heart disease	1,749 (54.1)	483 (32.2)	<0.001
Cardiomyopathy	638 (19.7)	284 (18.9)	0.533
Valvular heart disease	263 (8.1)	235 (15.6)	<0.001
Hypertensive heart disease	193 (6.0)	90 (6.0)	<1.000
Risk factors			
Hypertension	2,518 (77.9)	1,154 (76.8)	0.441
Diabetes mellitus	1,176 (36.4)	476 (31.7)	0.002
Dyslipidemia	2,371 (73.3)	1,062 (70.7)	0.066
Smoking	713 (23.4)	92 (6.6)	<0.001
Previous history			
Myocardial infarction	1,304 (40.3)	299 (19.9)	<0.001
Cerebral infarction	114 (3.5)	55 (3.7)	0.879
Atrial fibrillation	1,055 (32.9)	516 (34.7)	0.231
Malignant diseases	399 (12.3)	155 (10.3)	0.049
Hemodynamics and LV function			
SBP (mmHg)	126.1±18.9	126.7±19.8	0.32
DBP (mmHg)	72.7±11.8	71.2±12.2	<0.001
Heart rate (beats/min)	71.7±14.6	74.1±15.5	<0.001
LVDd (mm)	53.6±9	48.8±8.9	<0.001
LVEF (%)	55.5±15.2	60±15.4	<0.001
LVEF≥50%	2,041 (65.8)	1,083 (75.1)	<0.001
Laboratory findings			
Hemoglobin (g/dl)	13.6±2	12.3±2.2	<0.001
BUN (mg/dl)	20±10.4	20.3±10.8	0.337
Creatinine (mg/dl)	1.1±0.9	0.9±0.7	<0.001
Albumin (mg/dl)	4.1±0.5	4±0.5	<0.001
LDL-C (mg/dl)	103.5±30.6	108.3±31	<0.001
eGFR (ml·min^{-1}·1.73m^{-2})	61.6±24.5	58.3±22.8	<0.001
BNP (pg/ml)	184.7±275.6	219.6±323.8	<0.001

Data given as mean±SD or n (%).
BNP, brain natriuretic peptide; BUN, blood urea nitrogen; DBP, diastolic blood pressure; eGFR, estimated glomerular filtration rate; LDL-C, low-density lipoprotein cholesterol; LV, left ventricular; LVDd, left ventricular diastolic dimension; LVEF, left ventricular ejection fraction; NYHA, New York Heart Association; SBP, systolic blood pressure.

which 10,219 patients have been enrolled in the Tohoku district, Japan (NCT 00418041).[13–16]

Methods

CHART-2 Study

Details of the CHART-2 study have been described previously.[13–16] Briefly, the CHART-2 study is a multicenter, prospective observational study, in which 10,219 patients >20 years of age with significant coronary artery disease (stage A) and those in stages B–D HF were enrolled between October 2006 and March 2010.[13–16] All information, including medical history, laboratory data, and echocardiography data, were recorded at the time of enrollment, and thereafter annually by trained clinical research coordinators. Baseline cardiovascular disease, risk factors, and previous history were determined according to the data obtained from the case records at the time of enrollment. Valvular heart disease was defined as moderate to severe aortic and/or mitral valve disease without a previous history of valvular surgery, while hypertensive heart disease was defined as the presence of concentric hypertrophy (mean thickness of the ventricular septum and LV posterior wall ≥12mm) in patients with a history of hypertension but without a diagnosis of hypertrophic cardiomyopathy. The CHART-2 study was approved by the local ethics committee in each participating hospital and informed consent was obtained from all patients.

Table 2. Past History and Medication

	Male (n=3,234)	Female (n=1,502)	P-value
Past history			
PCI	1,231 (38.1)	304 (20.2)	<0.001
CABG	344 (10.6)	86 (5.7)	<0.001
ICD/CRT implantation	111 (3.4)	37 (2.5)	0.009
Other pacemaker implantation	209 (6.5)	165 (11)	<0.001
Medications			
Aspirin	2,016 (62.3)	706 (47)	<0.001
β-blocker	1,659 (51.3)	660 (43.9)	<0.001
RAS inhibitor	2,542 (78.6)	1,148 (76.4)	0.101
Diuretics	1,609 (49.8)	897 (59.7)	0.001
Calcium channel blocker	1,243 (38.4)	588 (39.1)	0.662
Statin	1,271 (39.3)	532 (35.4)	0.011

Data given as n (%).
CABG, coronary artery bypass grafting; CRT, cardiac resynchronization therapy; ICD, implantable cardioverter defibrillator; PCI, percutaneous coronary intervention; RAS, renin-angiotensin system.

Study Design

Among the 10,219 patients enrolled, 4,736 had HF in stage C/D. Stages A–D were defined at the time of registration in the CHART-2 study, according to the ACC/AHA guidelines classification:[17] stage A, at high risk for HF but without structural heart disease or symptoms of HF; stage B, structural heart disease but without signs or symptoms of HF; stage C, structural heart disease with prior or current symptoms of HF; and stage D, refractory HF requiring specialized interventions. The diagnosis of HF was made based on the criteria of the Framingham study.[1] Among the 4,736 stage C/D patients, 3,234 (68%) were male and 1,502 (32%) were female. Using the registry data of these patients, we examined gender differences in terms of clinical characteristics, management and long-term outcome in patients with stage C/D HF.

Statistical Analysis

All continuous variables are shown as mean±SD. Clinical characteristics of female and male patients were compared using Welch's t-test and Fisher's exact test with 2-sided P-values. Primary outcome measures of survival and HF-free survival were estimated by the Kaplan-Meier curve, and tested by the log-rank test in both genders. Incidence rates per 1,000 person-years for all-cause death, modes of death, HF requiring admission, acute myocardial infarction (AMI) and stroke were compared with the exact binominal test. Determinants of all-cause death were examined by the multivariate Cox proportional hazard model. Potential confounding factors with regard to baseline characteristics and treatments were included in multivariate analysis. The covariates for the multivariate analysis included gender, age, body mass index (BMI), history of hypertension, diabetes mellitus, dyslipidemia, and smoking, LVEF, systolic blood pressure (SBP), heart rate, hemoglobin, serum creatinine and brain natriuretic peptide (BNP) and treatment with β-blocker, renin-angiotensin system inhibitor (RASI) and statin. Interactions of gender and subgroups were estimated by the Cox proportional hazard model including interaction terms using the same variables listed here. Continuous variables were transformed into binary variables for estimation of interactions in the Cox model. P<0.05 and P-value for interaction <0.1 were considered as statistically significant in the present study. Statistical analysis was performed using IBM SPSS Statistics version 19 (IBM, Armonk, NY, USA) and R version 3.0.2.

Results

Baseline Characteristics

Baseline characteristics are listed in Table 1. Among the 4,736 Stage C/D patients, 1,502 (32%) were female and were 3.8 years older than men. Compared with men, women were more likely to be less obese, and were characterized by lower prevalence of ischemic heart disease, and had higher prevalence of valvular heart disease. In contrast, the prevalences of diabetes, smoking, MI and malignant disease were lower in women than in men. Although women had a higher prevalence of preserved LV function, they had relatively severe manifestation of CHF compared with men, including higher heart rate, higher NYHA class and increased BNP level. Baseline information regarding CHF treatment at the time of registration is given in Table 2. Women were less frequently treated with aspirin, β-blocker and statin, but more frequently with diuretics. In accordance with the lower prevalence of ischemic heart disease, women were less likely to undergo percutaneous coronary intervention or coronary artery bypass grafting. Furthermore, women were less frequently treated with implantable cardioverter defibrillator and/or cardiac resynchronization therapy, while more frequently treated with other cardiac pacemaker.

Gender Differences in Long-Term Outcome

There were 674 deaths during a median follow-up of 3.8 years, of which 338 (50.1%), 285 (42.3%), and 51 (7.7%) were due to cardiovascular, non-cardiovascular and unknown causes, respectively. Incidence of all-cause death was similar between the genders (52.4/1,000 vs. 47.3/1,000 person-years for women and men, respectively, P=0.225; Figures 1,2). Incidences of CHF requiring admission, AMI and stroke were also similar between the genders (Figure 2). As shown in Figure 3, women had higher cardiovascular mortality than men, particularly that due to HF, while men died more frequently of cancer. Although incidence of all-cause death was similar between the genders, multivariate Cox regression analysis revealed that women had a reduced risk of all-cause events than men after adjustment for clinical variables (hazard ratio [HR], 0.791; 95% confidence interval (95% CI): 0.640–0.9798, P=0.031), while it was not evident for cardiovascular death (HR, 1.027; 95% CI: 0.767–1.374, P=0.859) or HF requiring hospitalization (HR 0.858; 95% CI: 0.701–1.051, P=0.139; Table 3). Subgroup anal-